The Lees Approach to *Applied Mechanical Stabilization*™

Calling on our years of experience in research and application and combining this with our engineering expertise, Tensar brings you a whole new approach to road and rail foundation design. More scientifically rigorous and powerful than earlier methods, it has greater robustness and reliability across a wide range of applications and brings a whole new level of design capability. Best of all, we can introduce the benefits of mechanical stabilization more accurately than ever before, maximizing the benefit across all your projects.

Unpaved roads

Introduction

Unpaved roads are those constructed of a layer of unbound aggregate laid directly onto the existing ground or subgrade. They are called "unpaved" due to the absence of a permanent surface course, e.g., asphalt (flexible pavement) or cement concrete (rigid pavement), and the wheels of vehicles are supported directly on the aggregate.

The objective of the design method is straightforward: given a wheel load *P* passing *N* times along a proposed road, and a subgrade soil of a certain strength (often expressed as a California bearing ratio (CBR), what thickness *H* aggregate layer is needed to prevent excessive deformation of the road, as illustrated in Figure 1.

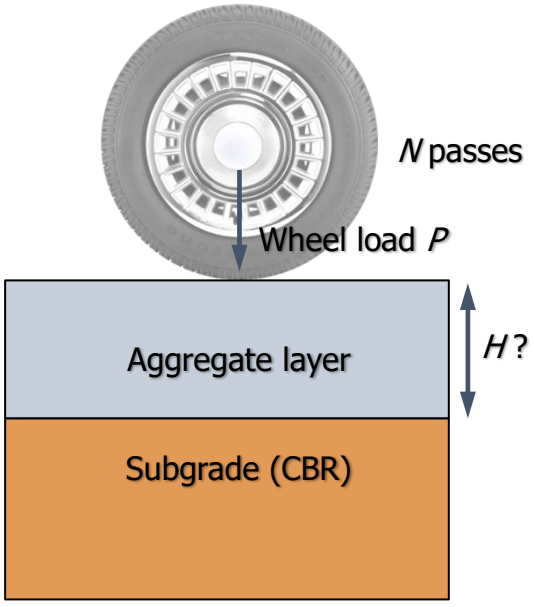

Figure 1: Objective of the design method

Deformation is usually expressed as a rut depth and if it becomes too large, the passage of vehicles may be hindered. Excessive deformation also leads to a more rapid deterioration of the road because it can lead to poor drainage.

Existing design methods have tended to be based on a narrow set of observations or required major assumptions that have restricted their range of application. The new Lees Approach to Applied Mechanical Stabilization (LAAMS) design method has overcome these shortcomings by characterizing the problem in terms of its true mechanics, based on extensive laboratory and small-scale and full-scale field testing. This has led to the development of new approaches to the calculation of tire contact area, bearing capacity, surface rutting and elastic deformation as well as incorporating the effect of wheel wander, as set out in this document.

Tire contact area

Traditionally, the wheel load is assumed distributed to the road surface as a uniformly distributed vertical stress equal to the tire inflation pressure and the contact area is assumed to be circular. This approach works reasonably well to determine the average contact stress on paved surfaces but, on unpaved roads, tire inflation pressures typically exceed the yield stress of unbound aggregates – more so, recently, as truck tire inflation pressures have increased due to improvements in tire technology.

Tire contact areas on unbound aggregate were investigated recently at the US Army Engineer Research and Development Center (ERDC) in Vicksburg, Mississippi. A dual-wheel with all combinations of either 10.3 or 6.6 kips (45.8 or 29.3 kN) wheel load (P) and tire inflation pressure (p) of either 100 or 120 psi (689 or 827 kPa) was driven onto and parked on a compacted, typical, road base aggregate. Contact areas were determined by spraying paint around the base of the tire and subsequently measuring the unpainted area beneath the tire.

The measured contact areas and corresponding calculated average contact stress are shown in Figure 2. The average contact pressures were much lower than the tire inflation pressures and the corresponding contact areas much larger than predicted by the traditional method. Assuming the contact width equals the tire width, more accurate predictions were obtained by calculating the contact length when the wheel load equals the surface bearing capacity of the unbound aggregate, as shown in Figure 2.

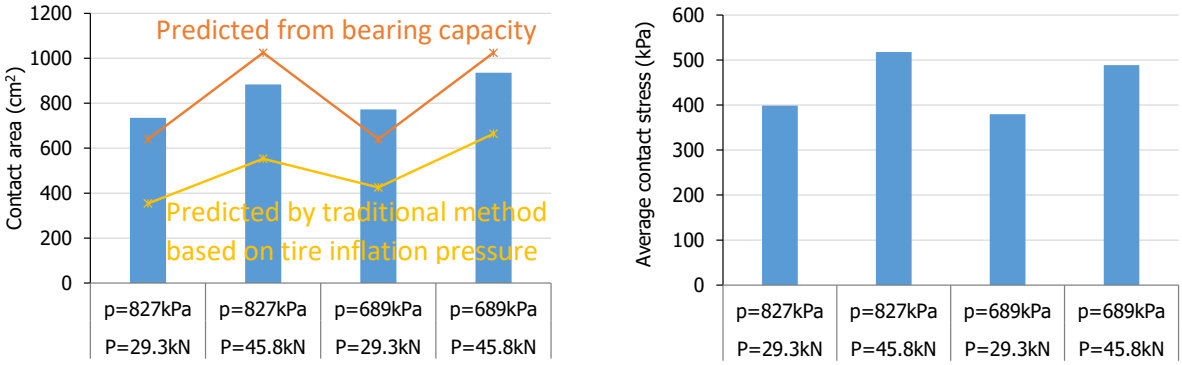

Figure 2: Measured tire contact areas on unbound aggregate

This is the proposed method to calculate the contact area when the tire inflation pressure exceeds the bearing capacity and the ground surface yields until the contact area is sufficiently large to just support the wheel load. The bearing capacity was calculated using the standard Terzaghi equation for surface foundations on cohesionless soils (Equation 1).

$$q_u = \frac{1}{2} B \gamma N_\gamma s_\gamma \quad (1)$$

Traditional formulas for the bearing capacity factor N_γ and shape factor s_γ tend to become inaccurate at the high φ' values (>40°) appropriate for high quality aggregates. Therefore, the formulas proposed by Loukidis and Salgado (2009) were adopted here, as given in Equations 2 and 3.

$$N_\gamma = \left(\frac{1+\sin\varphi}{1-\sin\varphi} e^{(1-0.13\tan\varphi)\pi\tan\varphi} - 1\right)\tan(1.34\varphi) \quad \text{assuming } \psi=\varphi\text{-}30° \quad (2)$$

$$s_\gamma = 1 + \frac{B}{L}\left(0.26\frac{1+\sin\varphi}{1-\sin\varphi} - 0.73\right) \quad (3)$$

The tire contact area study showed that the tire width (or, specifically, the tire tread width) determines the contact area dimension perpendicular to the direction of travel while the contact area dimension in the direction of travel increases with tire load as the unbound aggregate surface yields until there is sufficient bearing capacity to support the tire load. Therefore, the tire width is an input parameter to the calculation and the output is the tire contact length in the direction of travel, giving the overall rectangular contact area.

The tire contact area is assumed equal to the tire inflation pressure when it is less than the bearing capacity and the corresponding contact area is determined from the tire load. The tire contact area is still assumed to be rectangular with a width equal to the tire width and the required length to achieve the calculated contact area.

Permanent settlement

Existing design methods either implicitly or explicitly consider subgrade settlement only and assume that surface settlements match subgrade settlements with no contribution from the aggregate layer. This approach works reasonably well for soft subgrade cases where subgrade settlement accounts for the majority of surface settlement. However, as subgrades become stronger, deformations within the aggregate layer contribute to a greater proportion of surface settlement.

With the LAAMS method, contributions to surface settlement from both subgrade settlement s_T and aggregate layer deformation s_g are calculated separately and summed to obtain the surface settlement, as illustrated in Figure 3. As such, the method can be applied to a wider set of conditions, including those with a relatively high strength subgrade where aggregate layer deformations become important. Furthermore, since permanent deformations accumulate at different rates under trafficking in the two layers due to their different characteristics, treating the deformations separately increases the accuracy of surface settlement predictions under repeated traffic loads.

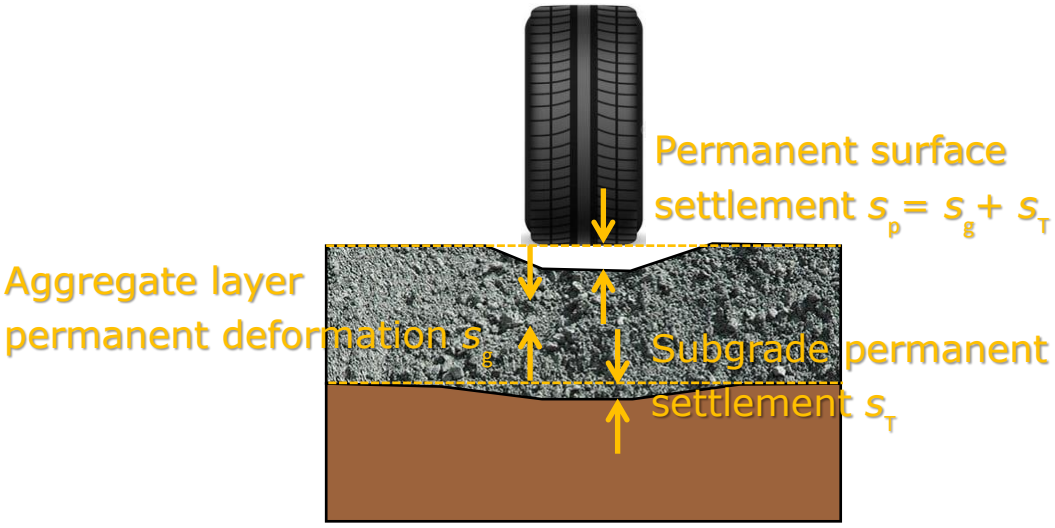

Figure 3: The two components of permanent surface settlement

Subgrade permanent settlement is also a useful output from the calculation since it provides an indication of the likelihood of water ponding on the subgrade surface. Ponding of water leads to subgrade deterioration, increased deformation and, overall, shortens the design life of the road. Moreover, it is harder to detect and repair subgrade settlement than surface settlement. This feature has allowed the introduction of different subgrade protection levels so that designers can choose to create an enhanced design to help extend design life and reduce maintenance.

The calculation of permanent settlement in each layer is undertaken in two stages. The permanent settlement on the first loading is calculated followed by its accumulation due to repetitions of the same loading, as described in the following sub-sections.

Permanent settlement on first loading

This method employs a settlement calculation approach used in geotechnical foundation design based on mobilized bearing capacity. This is a ratio between the mobilized to the total bearing capacity of the aggregate or the subgrade. It is particularly suited to the prediction of permanent (plastic) settlement which depends primarily on soil strength mobilization. Mobilization of the aggregate layer and subgrade (punching shear) bearing capacities are expressed as a ratio (M_g and M_T respectively) where zero means no load is applied and a value of 1 means full mobilization of bearing capacity (i.e., a mechanism with infinite permanent settlement).

Calculation of the aggregate layer mobilised bearing capacity ratio M_g first requires the calculation of the ultimate bearing capacity q_g of the aggregate layer for the tire contact area geometry. This is calculated using a modified form of Terzaghi's bearing capacity equation (Equation 4). The self-weight N_γ component of bearing capacity is normally multiplied by the average self-weight stress assumed to occur at a depth of $0.5B$. However, in this two-layer case, the base of the aggregate layer may lie deeper than the full assumed influence extent of the loading ($H>B$) or within it ($H<B$) which complicates the estimation of average overburden stress. Furthermore, the estimation of permanent aggregate deformation from M_g will also be influenced by the layer thickness H – thin layers will have less scope for deformation than thick

layers. Both of these issues were overcome by determining the overburden stress at the base of the layer (by replacing $0.5B$ with H in Equation 4) and by normalizing the aggregate permanent deformation s_g by H. Although this results in very high q_g values for thick layers, this is counterbalanced by relating the corresponding low M_g value to s_g/H and appears to fit the physical data well in the back-analysis of trafficking trials.

$$q_g = H\gamma N_\gamma s_\gamma \quad (4)$$

In contrast to the tire contact area calculations where the rectangular contact area dimensions followed the convention of $B \leq L$, wheel path deformations are constrained into a plane strain pattern perpendicular to the direction of wheel travel. As a result, the B dimension equals the tire width even when this is larger than the tire contact length, as illustrated in Figure 4. The B dimension is given the g subscript thus, B_g, to distinguish it from the B value adopted in subgrade deformation calculations which will differ in dual wheel cases.

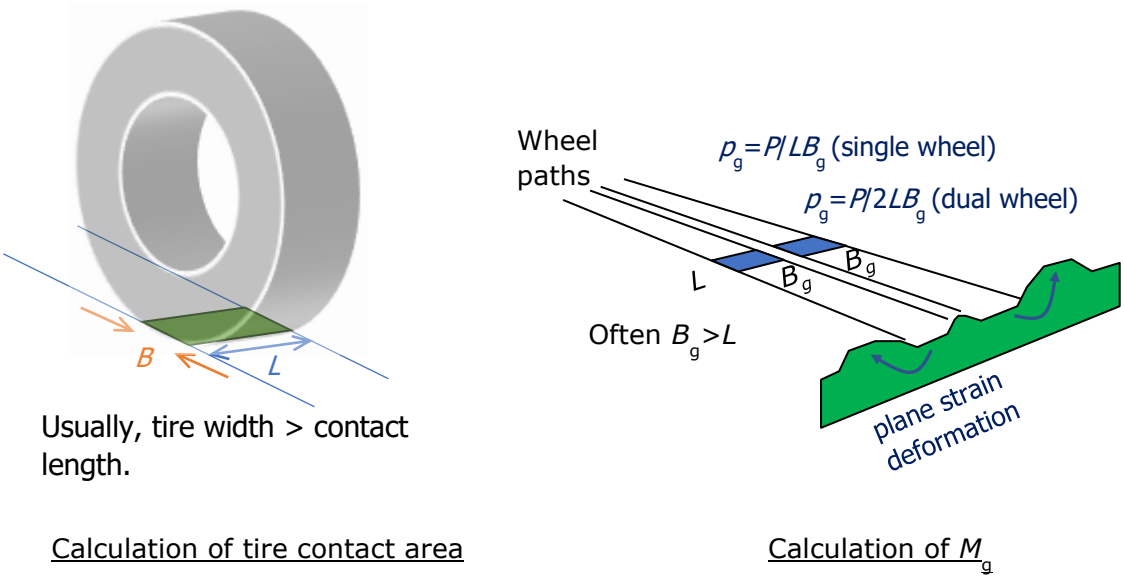

Figure 4: B and L conventions in tire contact area and M_g calculations

The hyperbolic relationship shown in Equation 5 and illustrated in Figure 5 allows the component of aggregate deformation $s_{g,N=1}$ that contributes to permanent surface settlement to be estimated. It has been derived from the back-analysis of cyclic plate load tests and full-scale trafficking tests. The value 1.05 instead of 1.0 appears in the denominator in recognition of the fact that even when the bearing capacity of the aggregate is fully mobilized (M_g=1), a mechanism does not form because as a wheel sinks into the aggregate its contact area increases and hence the contact stress reduces.

$$\frac{s_{g,N=1}}{H} = \frac{M_g^{1.45}}{38\left(1.05 - M_g\right)^{0.75}} \quad (5)$$

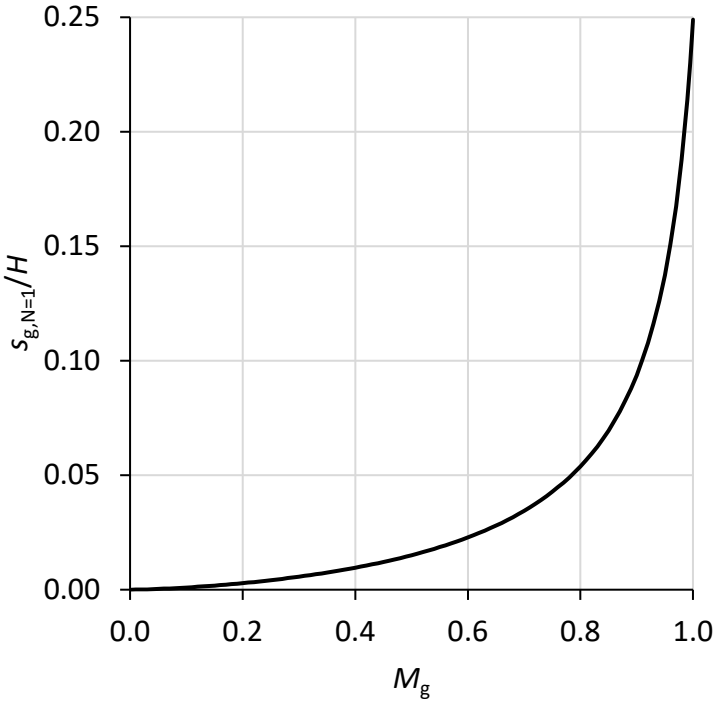

Figure 5: Hyperbolic relationship between mobilized bearing capacity and permanent aggregate deformation

Bearing capacity failure in the subgrade occurs by punching shear through the aggregate layer and a classical bearing capacity shear mechanism in the underlying subgrade, as illustrated in Figure 6. Lees (2020) derived the simple but versatile Equations 6 and 7 to determine the ratio q_T/q_s based on H/B_T and a load transfer efficiency T of the granular layer that depends on the strength ratio between the upper and lower layers. It was validated using the results of a literature review of centrifuge model testing and numerical analyses. It has also been adapted to include the benefits of mechanical stabilization in the upper granular layer. Refer to the working platform design approach document for more information.

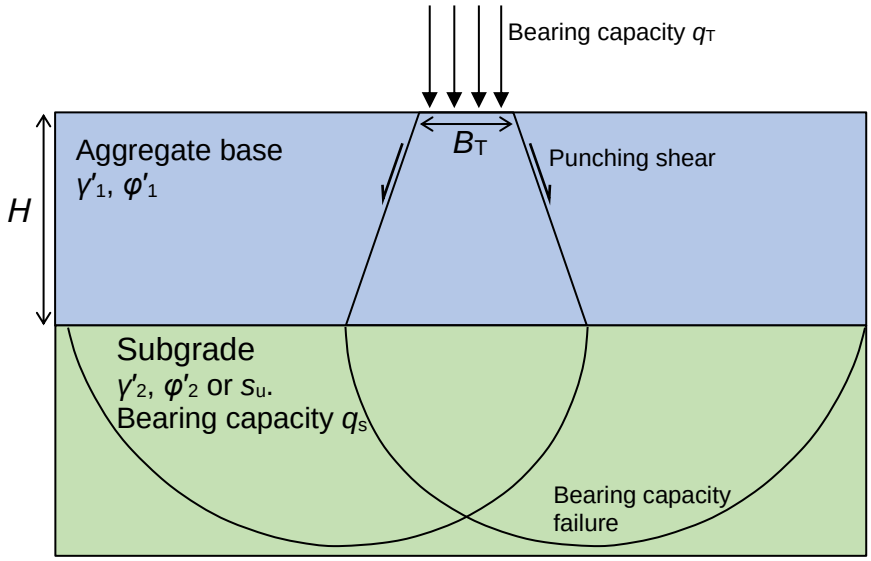

Figure 6: T-value method to determine subgrade bearing capacity

$$\frac{q_T}{q_s} = 1 + T\frac{H}{B_T} \quad \text{(strip footing)} \quad (6)$$

$$\frac{q_T}{q_s} = \left(1 + T\frac{H}{B_T}\right)^2 \quad \text{(square or circular footing)} \quad (7)$$

The strip (B_T/L=0) and square (B_T/L=1) bearing capacities are calculated using Equations 6 and 7 respectively and then the bearing capacity for any intermediate value of B_T/L obtained by linear interpolation. The loaded width B_T equals the tire width in single wheel cases but the full dual tire width in dual wheel cases since the effects of the two tires merge into one once the load is distributed down through the aggregate layer.

The subgrade permanent deformations are constrained into a plane strain pattern perpendicular to the direction of wheel travel. As a result, the B_T dimension equals the single or dual tire width even when this is larger than the tire contact length, as illustrated in Figure 7.

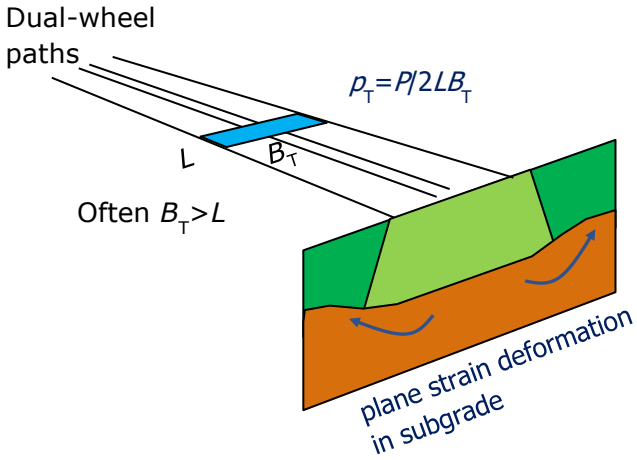

Figure 7: *B* and *L* conventions in tire contact area and M_T calculations

The hyperbolic relationship shown in Equation 8 and illustrated in Figure 8 allows the component of subgrade permanent settlement $s_{T,N=1}$ that contributes to permanent surface settlement to be estimated. It has been derived from the back-analysis of cyclic plate load tests and full-scale trafficking tests. The deformation accumulation model described in the following section assumes a continuous decay in the rate of accumulation which occurs provided that the subgrade mobilization stays below a threshold level of M_T=0.5.

$$\frac{s_{T,N=1}}{B_T} = \frac{M_T^{1.5}}{82(1-M_T)^2} \quad (8)$$

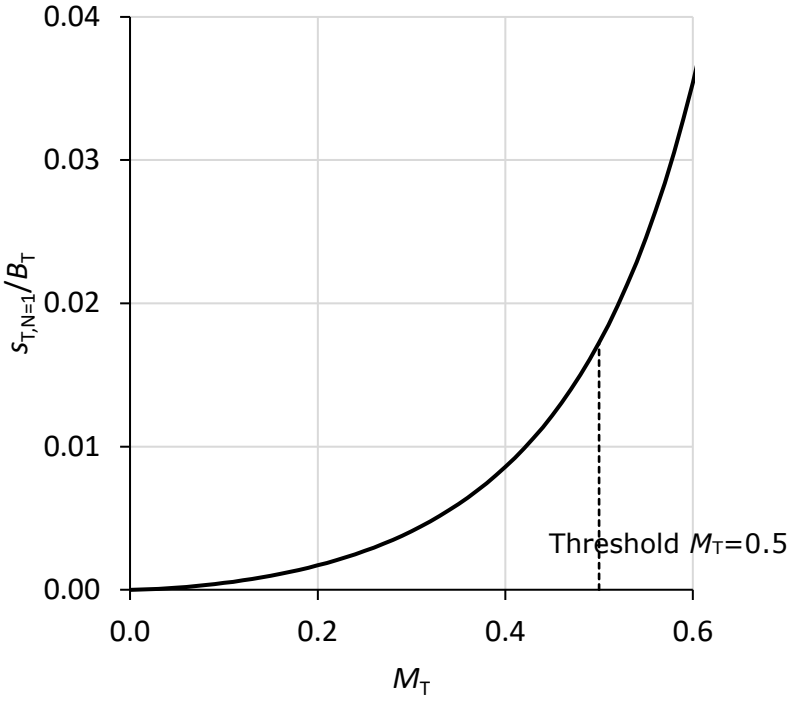

Figure 8: Hyperbolic relationship between mobilized bearing capacity and permanent settlement in cohesive subgrade

Permanent settlement accumulation

Many relationships have been proposed to characterise the accumulation of permanent deformation in various soil types. Perhaps the two simplest are Equations 9 and 10 which tend to be used for granular and cohesive soils respectively. They are also illustrated in Figure 9.

$$\varepsilon_p = A + B \ln N \quad (9)$$

$$\varepsilon_p = C N^d \quad (10)$$

ε_p is a plastic or permanent strain and is N is a whole positive number of identical load repetitions. Hence, both A and C equal the plastic strain following the first cycle of loading when N=1. The subsequent accumulation of permanent deformation with load repetitions is defined logarithmically with a B parameter in Equation 9 and according to a power law expression with parameter d in Equation 10. These tend to be derived from and validated against repeated load triaxial (RLT) tests undertaken up to around 10,000 cycles. Tests taken to a much higher number of load cycles show a slowing accumulation rate with respect to log$N$ at high N values which could lead to an overprediction of permanent deformations using Equations 9 and 10.

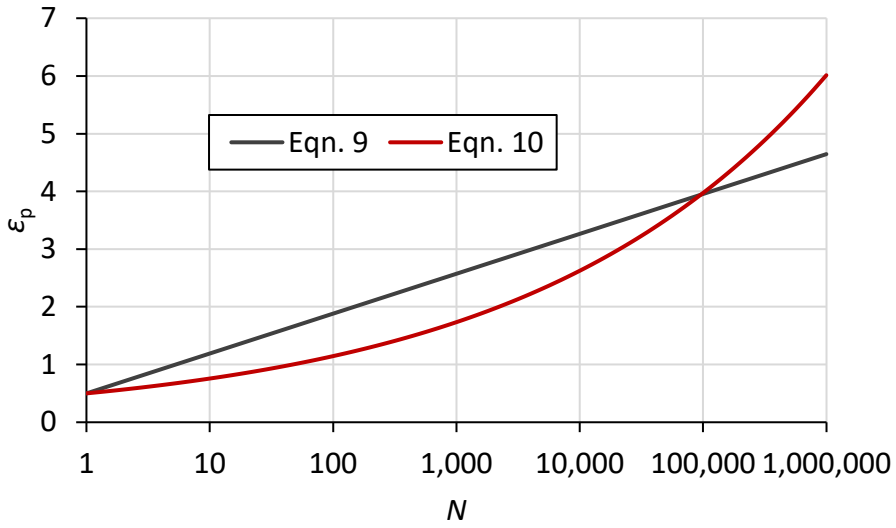

Figure 9: Simple permanent deformation accumulation models compared

A new, unifying expression for all soil types to predict the accumulation of permanent surface settlement under a repetitive load was derived as shown in Figure 10 and Equation 11. It is expressed as a ratio of the permanent settlement on first loading hence begins at 1 when N=1 (ln$N$=0). It increases with load repetitions towards an eventual maximum value (1+α) where α is the maximum permanent strain that can occur following the first load cycle. The maximum rate of growth with respect to ln$N$ occurs when half of α has accumulated and the number of load repetitions required to reach that point is defined by the β

parameter. It can be applied to most soil types once the alpha and beta values have been determined from cyclic triaxial testing to a high number of cycles (at least 10k for granular soils and 500k for cohesive soils).

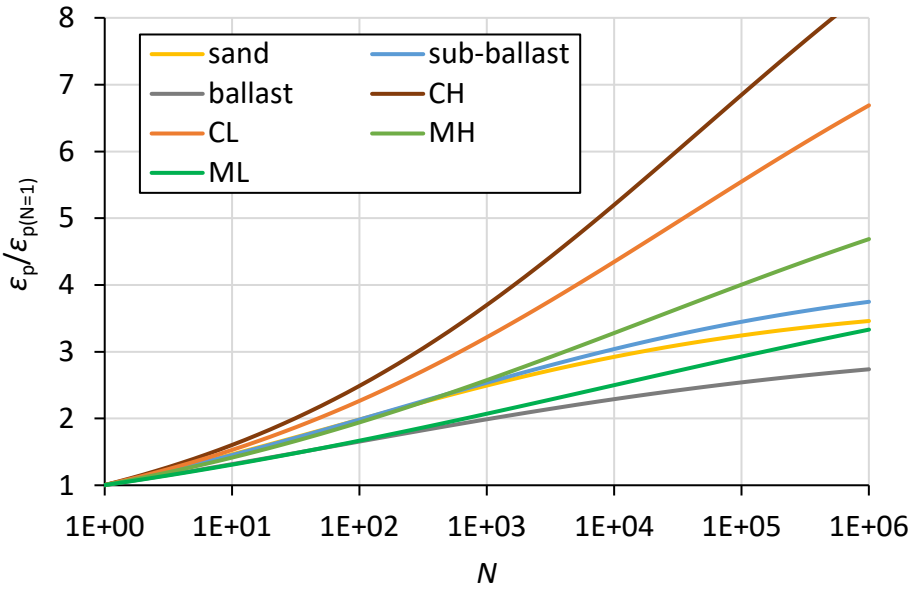

Figure 10: Permanent deformation accumulation model for all soil types

$$\frac{\varepsilon_p}{\varepsilon_{p(N=1)}} = \frac{1+\alpha}{1+\alpha e^{-\beta \ln N}} \qquad (11)$$

Permanent settlement in high subgrade bearing capacity mobilization cases

The permanent deformation accumulation models described in the previous section are considered valid for cases with subgrade bearing capacity mobilization factor M_T below a threshold of 0.5, so as to prevent ratcheting deformation towards failure. However, observations show that unpaved roads may still withstand a relatively low number of axle passes before reaching unacceptable levels of deformation, even when M_T exceeds the threshold value.

These observations from a number of full-scale trafficking trials are presented in Figure 11 as the number of axle passes needed to reach a failure criterion of permanent subgrade settlement s_T normalized by tire width B_T of 0.25 (equivalent to 75 mm settlement under a 0.3 m wide load) plotted against M_T. It is apparent that full bearing capacity mobilization (M_T=1) results in the failure criterion being reached on just one pass, as would be expected, while the number of passes needed to reach s_T/B_T of 0.25 increases exponentially as M_T decreases towards the threshold value of 0.5, as approximated by the line and equation shown. Note that the threshold value may be increased in cases of mechanical stabilized aggregate.

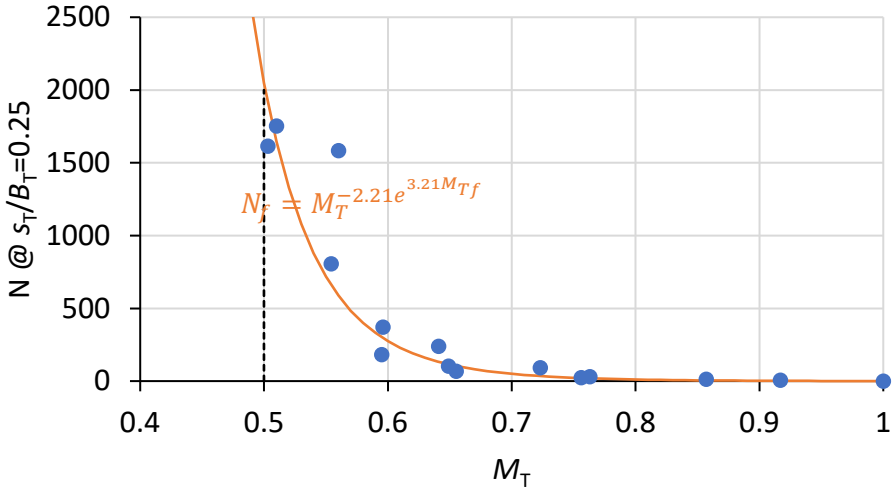

Figure 11: Unpaved road performance in high M_T cases

In design, the equation shown in Figure 11 is used to predict the number of axle passes N_f to reach the specified failure criterion (surface permanent settlement is assumed equal to subgrade permanent settlement in these high M_T cases). When the design number of axle passes N is greater than N_f, the aggregate thickness needs to be increased. When $N < N_f$, the thickness can be reduced or the accumulated permanent settlement is interpolated assuming a linear accumulation.

Wander

Both laboratory trafficking trials and existing design methods normally adopt or assume channelized traffic, i.e. each wheel pass follows the same path as the previous one. This leads to rutting along a distinct, narrow path. In practice, successive vehicles do not follow precisely the same wheel path. There is lateral variation, or wander, in the path each side of a mean wheel path as defined in Figure 8. The rutting calculation proposed in this document also assumes channelized traffic, but a means of correcting the number of wandering axle passes to an equivalent number of channelized axle passes has been introduced as described in this section.

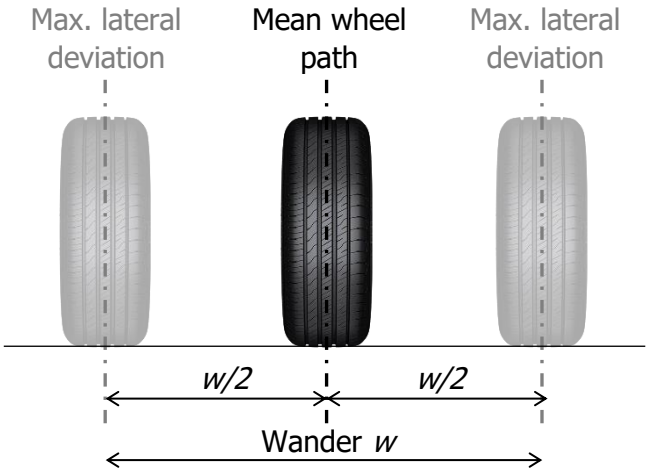

Figure 8: Definition of wander

The distribution of wheel paths about a mean would be expected to follow a normal distribution in most cases with the mean path having a wander of zero. There would be an equal chance of the wander occurring on each side of the mean and the largest wander to one side would, for practical purposes, represent 3 times the standard deviation σ of the distribution. Consequently, the wander w is equivalent to 6σ.

The maximum wheel path settlement along any unpaved road with a normally distributed wander would occur at the location of the mean wheel path (MWP). Therefore, the wheel path settlement prediction is made at this location with increments of settlement added for each equivalent channelized wheel pass (ECWP). Whenever the wheel's offset from the MWP is within half the tire width B either side of the MWP, one full ECWP is added.

When the offset is between 0.5 and 1.5 times the tire width, the wheel pass causes heave or a partial reversal of the MWP settlement. This is equivalent to a reduction in the number of wheel passes, so half an ECWP is subtracted. When the offset exceeds 1.5 times the tire width on either side, the wheel is so far from the MWP it is assumed that the wheel pass contributes no vertical displacement at all at the MWP.

The ECWP is summed for the specified number of wheel passes assuming they follow a normal distribution of wander about the MWP. Calculations of permanent settlement are then undertaken using the ECWP as the N value. The effect of wander on design outputs is often minor because settlement accumulates at a faster rate in the earlier passes than the later passes. Therefore, even when the ECWP is significantly less than the true number of wheel passes, a significant proportion of the uncorrected settlement still occurs during those equivalent channelized wheel passes. The larger the wander and the narrower the tire, the greater the difference on design outputs.

Converting permanent settlement to permanent rut depth

The calculations described so far provide outputs of permanent settlement, but rut depth is a more common and more useful performance criterion because this affects the trafficability of a road and the distinction

between the two is illustrated in Figure 9. Rut depth also makes a more suitable performance criterion for the subgrade because this directly corresponds with the water ponding depth that may occur. However, direct estimation of rut depth is more difficult because it depends on both the settlement under the wheel path and the heave that occurs to the sides of the wheel path due to shear deformation.

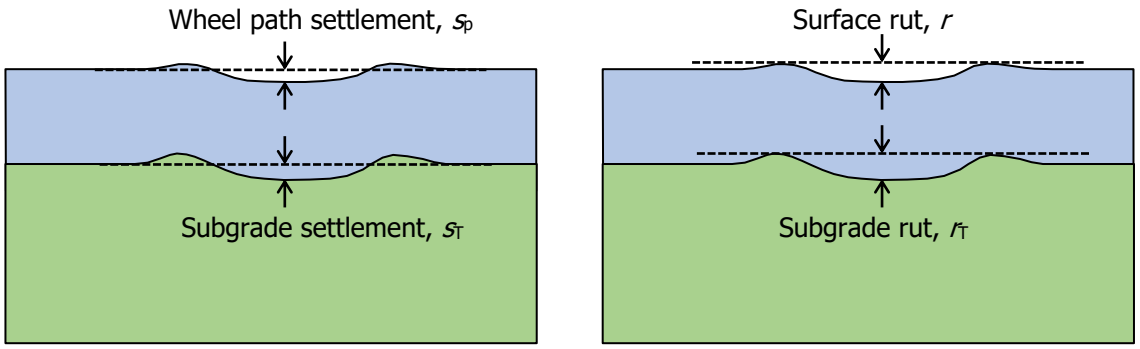

Figure 9: Distinguishing between settlement and rut depth

Measurements of wheel path settlement and rut depth from several full-scale trafficking trials on unpaved roads were analyzed to understand the relationship between rut and settlement. About 100 data points from post-test surveys of wheel path settlement and rut depth are plotted in Figure 10. Clear relationships were identified as shown by the red lines which are used to convert the calculation output of permanent settlement into rut depth.

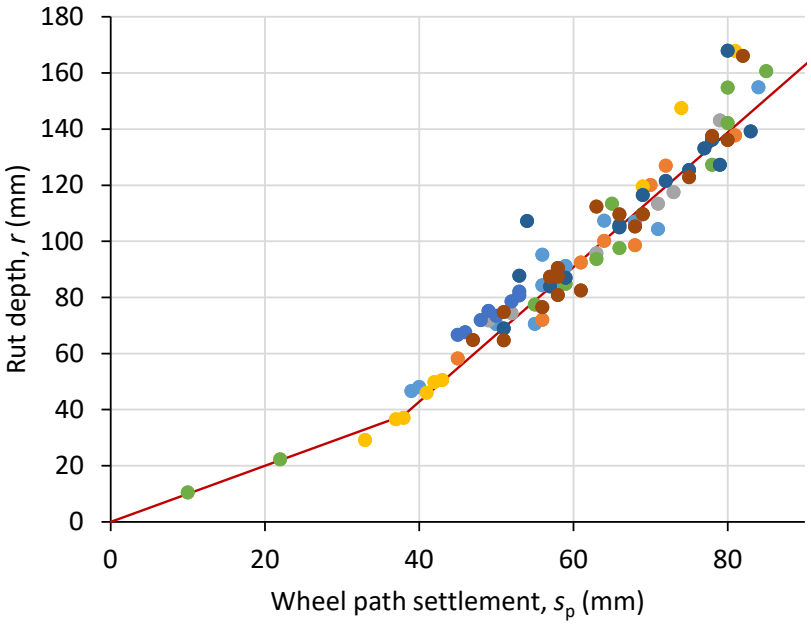

Figure 10: Measured surface settlement and rut depth from full-scale trafficking trials

The maximum permitted surface rut depth is set as an input parameter in the Tensar+ module for unpaved roads. The program then determines the minimum required aggregate layer thickness to reach the

specified rut depth under the specified traffic loading. On some occasions, the aggregate layer thickness may need to be increased to achieve adequate factor of safety against bearing capacity failure which will be indicated in the output and consequently the predicted surface rut depth may be less than the specified value.

Additionally, users may select from three subgrade protection levels appropriate for different applications as shown in Table 1. These are met by ensuring the predicted subgrade rut depth satisfies the allowable values indicated. Higher subgrade protection levels may require the aggregate thickness to be increased over and above that required to satisfy the specified surface rut criterion.

Protection level	Allowable subgrade rut depth	Recommended applications	Risk of water ponding
Protected (best)	< 6 mm	Permanent high-volume roads or critical applications	Minimal
Improved (better)	6-12 mm	Permanent low-volume roads and less critical applications	Reduced
Adequate (good)	> 12 mm	Temporary access roads or non-critical applications	Possible

Table 1: Subgrade protection levels

The allowable subgrade rut depth values are those considered critical to the occurrence of water ponding on the subgrade surface and hence accelerated subgrade degradation. Values up to 6mm (1/4 in.) are considered within the tolerances of what can be achieved when preparing a subgrade surface during construction. Small, temporary ponding may occur but capillary rise within the aggregate layer would be expected to dry these. Subgrade rut depths in excess of 12mm (1/2 in.) would be expected to form significant ponding that cannot be dried by capillary rise in the aggregate and which may linger for long periods.

Elastic settlement

Elastic settlement concerns the entirely recoverable surface displacements that occur when wheels travel along an unpaved road surface and can be predicted relatively accurately under the assumption of linear elasticity. A parametric study using a linear elastic axisymmetric finite element analysis (FEA) model was undertaken with the loaded radius, aggregate thickness and stiffness properties of both layers all varied as shown in Figure 11. A typical Poisson's ratio ν_1 for the aggregate layer of 0.2 was adopted in all cases. Additional analyses were performed with ν_1 varied between 0.1 and 0.35 and the effect on predicted

settlement was less than ±5%. Given the uncertainty and difficulty of measuring ν, it is considered unnecessary to have it as an input parameter for the aggregate layer given its insignificant effect on outputs. ν_2 for the subgrade was taken as 0.5 (0.495 to be precise to avoid a singularity in the stiffness matrix) appropriate for an undrained soil (clay or silt) under transient traffic loading. The parametric study was repeated with ν_2 set at 0.2 which is appropriate for drained soils (sand) under transient loading. Again, outputs were not sensitive to small changes to ν_2 but the change from undrained (0.5) to drained (0.2) caused on average about an 8% change in settlement predictions.

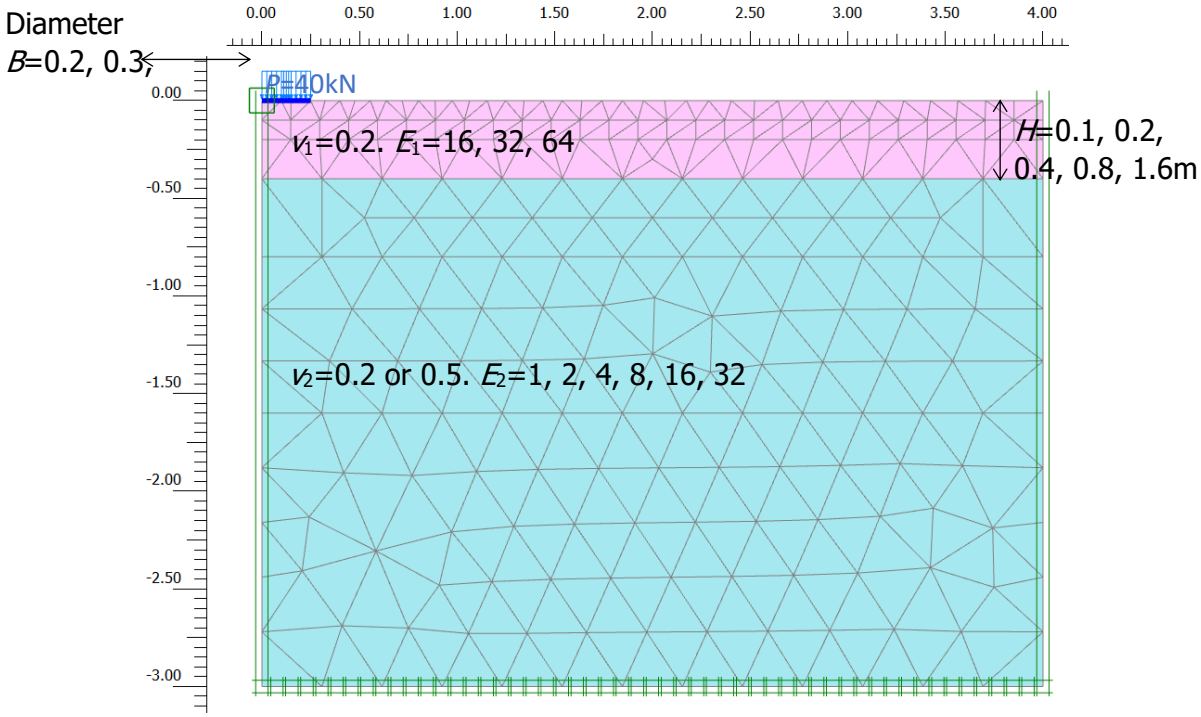

Figure 11: FEA model employed in elastic settlement parametric study

The outputs of vertical displacement s normalized by the plate diameter are plotted in Figures 12 and 13 for the undrained and drained subgrade conditions respectively. It was found that a good agreement could be obtained simply by predicting the displacement according to the equations shown and as plotted on the vertical axes. Therefore, these equations are used to provide a quick and simple means of predicting the elastic vertical displacement of an unpaved road on a homogeneous subgrade with a similar accuracy level to a linear elastic FEA model.

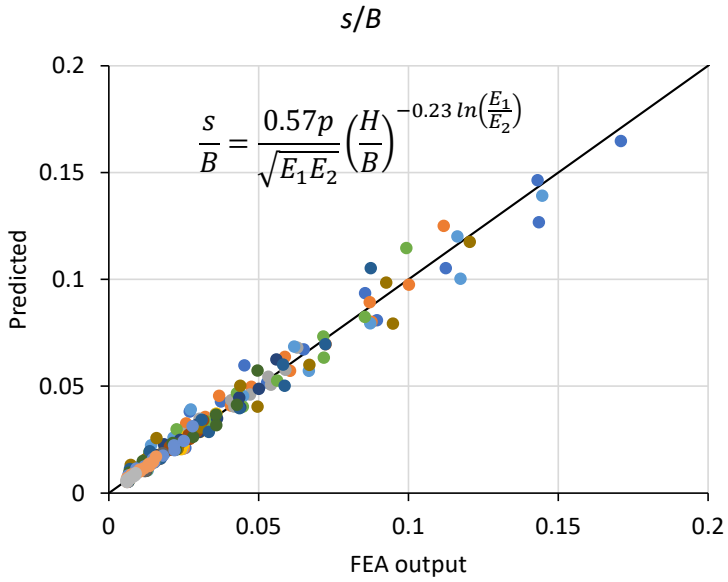

Figure 12: Elastic settlement FEA parametric study output for undrained subgrades

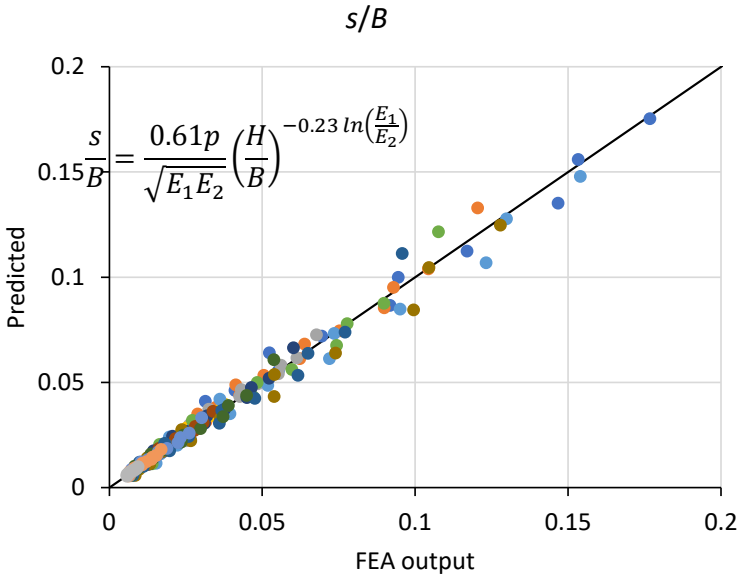

Figure 13: Elastic settlement FEA parametric study output for drained subgrades

This approach may be used to predict elastic settlements caused by traffic occurring on construction (during a proof roll, for example) or for long-term resilient settlements by using as-constructed and resilient moduli respectively.

The stiffness of aggregate layers as constructed can either be measured or estimated. It depends to a large extent on their relative density and hence compaction efficiency. This, in turn, depends on the strength and stiffness of the underlying subgrade. Accordingly, based on the improved bearing capacity predicted by the T-value method and field experience, a relationship for estimating the as-constructed stiffness of high-quality road base aggregates compacted by typical methods on different CBR subgrades were derived as shown in Figure 14. The subgrade stiffness E_2 is based either on measurement or estimated from appropriate correlations in the literature.

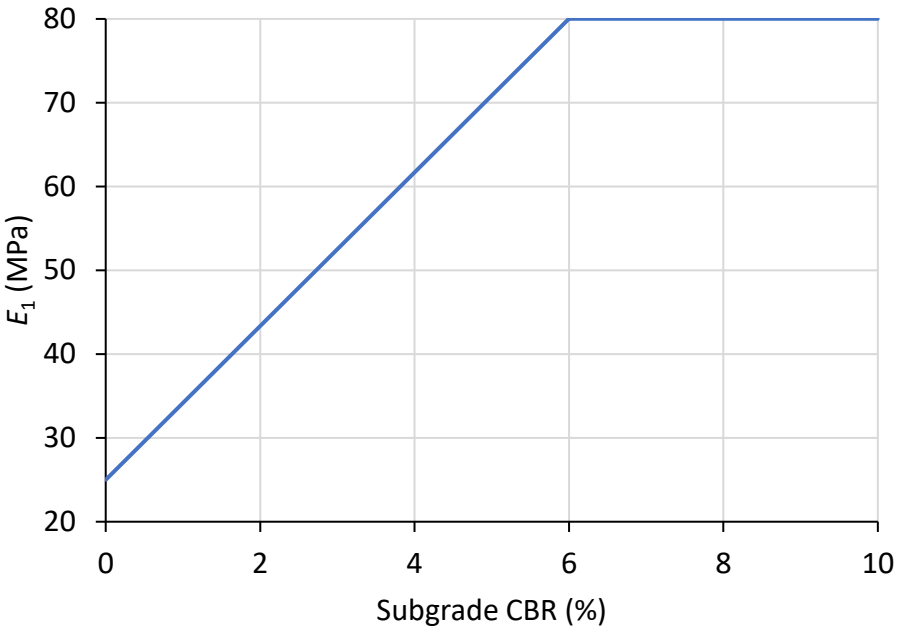

Figure 14: Estimated as-constructed road base stiffness on different CBR subgrades

With these values and traffic information it is possible to estimate the required aggregate layer thickness H to achieve a specified elastic settlement. Note that the effect of H on elastic settlement is non-linear because, as H increases, the subgrade stiffness E_2 has less influence on surface settlement. Hence, large changes in H may be needed to effect significant change in elastic settlement.

References

Lees AS (2020). The bearing capacity of a granular layer on clay, *Proceedings of the Institution of Civil Engineers – Geotechnical Engineering* **173**(1) 13–20.

Lees AS and Clausen J (2020). Strength envelope of granular soil stabilized by multi-axial geogrid in large triaxial tests, *Canadian Geotechnical Journal* **57**(3) 448-452.